

Research Article

Open Access

M. Davarpanah, G. Somodi, L. Kovács, B. Vásárhelyi*

Complex analysis of uniaxial compressive tests of the Mórágý granitic rock formation (Hungary)

<https://doi.org/10.2478/sgem-2019-0010>

received September 15, 2018; accepted February 4, 2019.

Abstract: Understanding the quality of intact rock is one of the most important parts of any engineering projects in the field of rock mechanics. The expression of correlations between the engineering properties of intact rock has always been the scope of experimental research, driven by the need to depict the actual behaviour of rock and to calculate most accurately the design parameters. To determine the behaviour of intact rock, the value of important mechanical parameters such as Young’s modulus (E), Poisson’s ratio (ν) and the strength of rock (σ_{cd}) was calculated. Recently, for modelling the behaviour of intact rock, the crack initiation stress (σ_{ci}) is another important parameter, together with the strain (ϵ). The ratio of Young’s modulus and the strength of rock is the modulus ratio (M_R), which can be used for calculations. These parameters are extensively used in rock engineering when the deformation of different structural elements of underground storage, caverns, tunnels or mining opening must be computed. The objective of this paper is to investigate the relationship between these parameters for Hungarian granitic rock samples. To achieve this goal, the modulus ratio ($M_R = E/\sigma_c$) of 50 granitic rocks collected from Bataapáti radioactive waste repository was examined. Fifty high-precision uniaxial compressive tests were conducted on strong ($\sigma_c > 100$ MPa) rock samples, exhibiting the wide range of elastic modulus ($E = 57.425\text{--}88.937$ GPa), uniaxial compressive strength ($\sigma_c = 133.34\text{--}213.04$ MPa) and Poisson’s ratio ($\nu = 0.18\text{--}0.32$). The observed value ($M_R = 326\text{--}597$) and mean value of $M_R = 439.4$ are compared with the results of similar previous researches. Moreover, the statistical analysis for all studied rocks was performed and the relationship

between M_R and other mechanical parameters such as maximum axial strain ($\epsilon_{a, \max}$) for studied rocks was discussed.

Keywords: uniaxial compressive test; modulus ratio (M_R); maximum axial strain ($\epsilon_{a, \max}$); crack damage stress (σ_{cd}); crack initiation stress (σ_{ci}); Mórágý granite formation.

1 Introduction

Rock engineering properties are considered to be the most important parameters in the design of groundworks. Two important mechanical parameters, uniaxial compressive strength (σ_c) and elastic modulus of rock (E), should be estimated correctly. There are different empirical relationships between σ_c and E obtained for limestones, agglomerates, dolomites, chalks, sandstones and basalts [1, 2, 3], among the others.

Hypothetical stress–strain curves for three different rocks are presented in Fig. 1 by Ramamurthy et al. [4]. Based on the figure, curves OA, OB and OC represent three stress–strain curves with failure occurring at A, B and C, respectively. According to their sample, curves OA and OB have the same modulus but different strengths and strains at failure, whereas the curves OA and OC have the same strength but different modulus and strains at failure. It means, neither strength nor modulus alone could be chosen to represent the overall quality of rock. Therefore, strength and modulus together will give a realistic understanding of the rock’s response to engineering usage. This approach of defining the quality of intact rocks was proposed by Deere and Miller [5] considering the modulus ratio (M_R), which is defined as the ratio of tangent modulus of intact rock (E) at 50% of failure strength and its compressive strength (σ_c).

The modulus ratio $M_R = E/\sigma_c$ between the modulus of elasticity (E) and uniaxial compressive strength (σ_c) for intact rock samples varies from 106 to 1,600 [6]. For most rocks, M_R is between 250 and 500 with average $M_R = 400$, $E = 400 \sigma_c$.

*Corresponding author: B. Vásárhelyi, Department of Engineering Geology and Geotechnics, Budapest University of Technology and Economics, Budapest, Hungary, E-mail: vasarhelyi.balazs@epito.bme.hu
 M. Davarpanah: Department of Engineering Geology and Geotechnics, Budapest University of Technology and Economics, Budapest, Hungary
 G. Somodi, L. Kovács: RockStudy Ltd., Pécs, Hungary

Palchik [7] examined the M_R values for 11 heterogeneous carbonate rocks from different regions of Israel. The investigated dolomites, limestones and chalks had weak to very strong strength with a wide range of elastic modulus. He found that M_R is closely related to the maximum axial strain ($\varepsilon_{a,max}$) at the uniaxial strength of the rock (σ_c) and the following relationship was found (Fig. 2):

$$M_R = \frac{2k}{\varepsilon_{a,max} (1 + e^{-\varepsilon_{a,max}})} \quad (1)$$

where k is the conversion coefficient equal to 100 and $\varepsilon_{a,max}$ is in %. When M_R is known, $\varepsilon_{a,max}$ (%) is obtained from Eq. (1) as

$$\varepsilon_{a,max} = \frac{k}{M_R - 0.46k} \quad (2)$$

The expansion of the expression $2/(1 + e^{-\varepsilon_{a,max}})$ using Taylor's theorem shows the value of $2/(1 + e^{-\varepsilon_{a,max}}) = 1 + 0.46 \varepsilon_{a,max}$ [8].

The goal of this paper is to check Eq. (1) for Hungarian granitic rocks as well as to study the relationships between characteristic compressive stress level, strain and mechanical properties. These granitic rock samples were investigated previously by Vászrhelyi et al. [8] using multiple failure state triaxial tests.

2 Laboratory investigations and analyses

Laboratory samples originated from research boreholes deepened in carboniferous Mórággy granite formation during the research and construction phases of deep geological repository of low- and intermediate-level radioactive waste. This granite formation is a carboniferous intruded and displaced Variscan granite pluton situated in South-West Hungary. The main rock types are mainly microcline megacryst-bearing, medium-grained, biotite monzogranites and quartz monzonites [9] (see Fig. 3). In spatial viewpoint, the monzogranitic rocks contain generally oval shaped, variably elongated monzonite enclaves (predominantly amphibole–biotite monzonites, diorites and syenites) of various sizes (from a few centimetre to several 100 metres) reflecting the mixing and mingling of two magmas with different composition. Feldspar quartz-rich leucocratic dykes

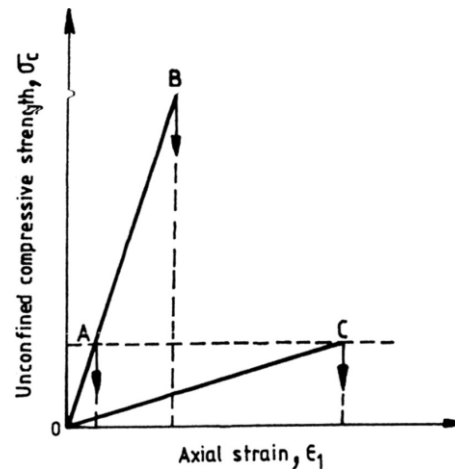


Figure 1: Hypothetical stress–strain curves [4].

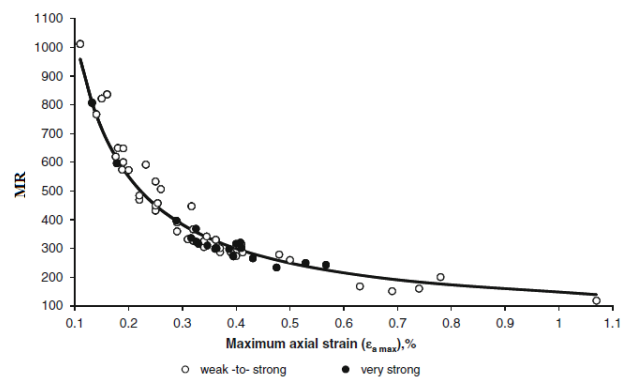


Figure 2: Relationship between modulus ratio (M_R) and maximum axial strain ($\varepsilon_{a,max}$) using different carbonate rocks [7].

belonging to the late-stage magmatic evolution and Late Cretaceous trachyte and tephrite dykes cross cut all of the previously described rock types [10]. In general, fractured but fresh rock is common which is sparsely intersected by fault zones with few metre thick clay gauges. Intense clay mineralisation in the fault cores indicates a low-grade hydrothermal alteration.

The samples were tested by using a computer-controlled servo-hydraulic machine in continuous load control mode. The magnitude of loading was settled in kilonewton with 0.01 accuracy, and the rate of loading was 0.6 kN/s. Axial and tangential deformation was measured by strain gauges, which measures the deformation between 1/4 and 3/4 of the sample's height.

Fifty uniaxial compressive tests were performed in the rock mechanics laboratory at RockStudy Ltd. The NX ($d = 50$ mm)-sized cylindrical rock samples having the ratio of $L/d = 2/1$ (here L and d are the length and diameter of a sample, respectively) were prepared (see

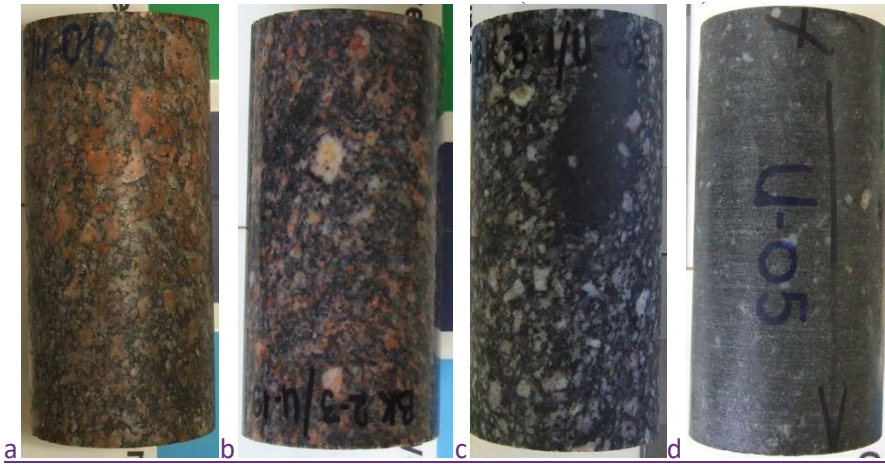


Figure 3: Main types of rock samples. (a, b) Megacryst-bearing, medium-grained, biotite monzogranites. (c) Medium-grained, biotite monzogranites with elongated monzonitic enclaves. (d) Quartz monzonite.



Figure 4: A prepared sample in the beginning of the UCS test.

Fig. 4). Mechanical properties of granitic rock samples are summarised in Table 1.

UCS, uniaxial compressive strength

Table 1 summarizes the value of elastic modulus (E), crack damage stress (σ_{cd}), uniaxial compressive strength (σ_c), Poisson’s ratio (ν), crack initiation stress (σ_{ci}), axial failure strain ($\epsilon_{a, max}$), maximum volumetric strain (ϵ_{cd}), crack initiation strain (ϵ_{ci}) and M_R for each of the studied 50 samples.

The values of elastic modulus (E) and Poisson’s ratio (ν) were calculated by using linear regressions along linear portions of stress–axial strain curves and radial strain–axial strain curves, respectively. The values of

crack initiation stress (σ_{ci}) and crack damage stress (σ_{cd}) were calculated based on the following methods:

2.1 Onset dilatancy method

In this method, [11], crack initiation threshold is visible on the axial–volumetric strain curve (Fig. 5) when it diverges from the straight line. In practice, small deviation of the stress–volumetric strain curve from the straight line can make some difficulties to define one point determining the threshold of crack initiation.

2.2 – Crack volumetric strain method

Martin and Chandler [12] proposed that crack initiation could be determined using a plot of crack volumetric strain versus axial strain (Fig. 6). Crack volumetric strain ϵ_{Vcr} is calculated as a difference between the elastic volumetric strain ϵ_{Vel} and volumetric strain ϵ_V determined in the test,

$$\epsilon_V = 2\epsilon_1 + \epsilon_a \tag{3}$$

$$\epsilon_{Vcr} = \epsilon_V - \epsilon_{Vel} \tag{4}$$

$$\epsilon_{Vel} = \frac{1-2\nu}{E}(\sigma_1 + 2\sigma_3) \tag{5}$$

ϵ_a and ϵ_1 are the axial and lateral strain; σ_1 and σ_3 are the axial and confining stress and E and ν are the Young’s modulus and Poisson’s ratio, respectively.

Table 1: Mechanical properties of investigated Mórágý granitic rock samples.

Rock sample	ν	E	ε_{ci}	σ_{ci}	ε_{cd}	σ_{cd}	$\varepsilon_{a,max}$	σ_c	M_R
(-)	(GPa)	(%)	(MPa)	(%)	(MPa)	(%)	(MPa)	(-)	
BeR-6_U-10	0.24	74.776	0.030	50.73	0.091	152.244	0.278	181.05	413.0
BeR-7_U-02	0.21	71.612	0.037	50.37	0.095	145.15	0.34	174.80	409.7
BeR-7_U-04	0.25	74.447	0.037	59.61	0.063	131.70	0.33	183.39	405.9
BeR-8_U-01	0.22	63.357	0.060	59.84	0.120	165.89	0.29	184.48	343.4
BeR-10_U-08	0.21	66.129	0.025	30.06	0.044	77.30	0.22	137.14	482.2
BeR-10_U-18	0.23	72.794	0.048	64.89	0.078	148.24	0.2	148.39	490.6
BeR-10_U-20	0.23	63.787	0.035	39.28	0.087	133.75	0.27	156.74	407.0
BeR-11_U-08	0.23	68.950	0.054	80.82	0.104	168.94	0.31	204.23	337.6
BeR-12_U-02	0.22	79.660	0.029	34.36	0.08	128.84	0.18	133.34	597.4
BK1-1_U-12	0.23	70.153	0.036	51.74	0.076	131.50	0.23	172.74	406.1
BK1-3_U-01	0.32	72.891	0.037	79.97	0.053	121.05	0.28	184.59	394.9
BK1-3_U-03	0.19	69.164	0.065	71.75	0.14	132.66	0.22	133.62	517.6
BK1-3_U-04	0.18	71.860	0.045	47.93	0.113	112.28	0.18	153.60	467.8
BK1-3_U-08	0.23	70.137	0.059	80.36	0.147	142.79	0.22	172.55	406.5
BK1-3_U-12	0.25	57.425	0.066	67.99	0.13	134.11	0.27	135.14	424.9
BK2-1_U-03	0.21	74.228	0.057	74.61	0.09	131.78	0.19	146.65	506.2
BK2-3_U-07	0.28	77.332	0.036	59.84	0.068	119.12	0.19	143.71	538.1
BK2-3_U-15	0.22	80.365	0.035	48.57	0.090	160.74	0.24	178.41	450.5
BK2-3_U-18	0.2	73.819	0.069	80.22	0.11	153.84	0.23	159.16	463.8
BK2-4_U-02	0.2	76.820	0.06	88.12	0.106	177.32	0.26	205.62	373.6
BK2-4_U-04	0.21	77.709	0.045	60.07	0.090	130.57	0.20	155.49	499.8
BK2-5_U-02	0.25	77.866	0.038	62.63	0.070	134.14	0.23	166.29	468.3
Bkf-1_U-03	0.24	77.665	0.050	50.46	0.070	120.14	0.30	161.63	480.5
Bkf-2_U-03	0.22	60.602	0.065	76.84	0.118	164.66	0.39	180.93	334.9
Bkf-4_U-03	0.22	79.856	0.042	60.29	0.083	142.38	0.24	179.28	445.4
Bkf-5_U-02	0.24	79.818	0.034	53.90	0.067	135.29	0.20	169.67	470.4
Bl-112_U-02	0.21	72.897	0.029	37.88	0.093	144.19	0.20	164.59	442.9
Bp-4_U-05	0.25	76.992	0.041	69.46	0.1	181.85	0.24	187.69	410.2
Bp-4B_U-01	0.21	69.800	0.042	49.25	0.109	159.85	0.36	184.45	378.4
Bp-4B_U-05	0.23	76.237	0.033	49.37	0.076	148.77	0.28	170.10	448.2
Bp-4B_U-13	0.27	77.924	0.049	74.11	0.096	170.28	0.25	177.91	438.0
Bp-4B_U-17	0.24	74.648	0.045	60.27	0.083	162.61	0.26	181.43	411.4
Bp-4B_U-19	0.22	77.182	0.058	80.43	0.100	160.13	0.25	190.48	405.2
Bp-4B_U-23	0.24	74.683	0.053	80.00	0.077	137.96	0.24	165.23	452.0
Bp-5_U-19	0.25	73.506	0.031	49.73	0.056	121.48	0.23	149.76	490.8
Bp-5_U-21	0.25	80.159	0.040	70.45	0.064	137.00	0.26	171.46	467.5
Bx-81_U-03	0.22	65.782	0.045	53.44	0.088	130.84	0.29	149.28	440.7
Bx-82_U-01	0.25	82.940	0.046	80.51	0.085	162.08	0.27	180.33	459.9
Bx-82_U-03	0.29	84.949	0.024	49.99	0.044	120.612	0.2	166.87	509.1
Bx-83_U-01	0.26	72.864	0.030	60.56	0.067	150.321	0.26	169.70	429.4
Bx-83_U-03	0.25	78.072	0.057	90.36	0.095	182.085	0.37	212.42	367.5
Bx-84_U-01	0.25	80.669	0.047	79.90	0.073	147.6	0.23	178.07	453.0

Continued **Table 1:** Mechanical properties of investigated Mórágý granitic rock samples.

Rock sample	ν	E	ε_{ci}	σ_{ci}	ε_{cd}	σ_{cd}	$\varepsilon_{a,max}$	σ_c	M_R
	(-)	(GPa)	(%)	(MPa)	(%)	(MPa)	(%)	(MPa)	(-)
Bx-84_U-03	0.27	81.144	0.039	69.38	0.062	138.183	0.26	166.94	486.1
Bx-101_U-02	0.24	76.994	0.042	71.53	0.058	112.5	0.19	142.49	540.3
Bx-101_U-04	0.26	79.300	0.048	60.58	0.091	160.96	0.23	163.19	485.9
Bz-921_U-01	0.21	71.574	0.056	68.79	0.121	164.573	0.3	192.80	371.2
Bz-942_U-01	0.23	73.511	0.053	73.43	0.11	182.66	0.28	198.58	370.2
Bz-1221_U-01	0.2	69.540	0.049	58.25	0.100	165.836	0.29	213.04	326.4
Bz-1311_U-01	0.3	88.937	0.035	75.93	0.060	163.371	0.23	206.48	430.7
Bz-1351_U-01	0.25	67.053	0.034	50.86	0.080	145.566	0.28	159.97	419.2

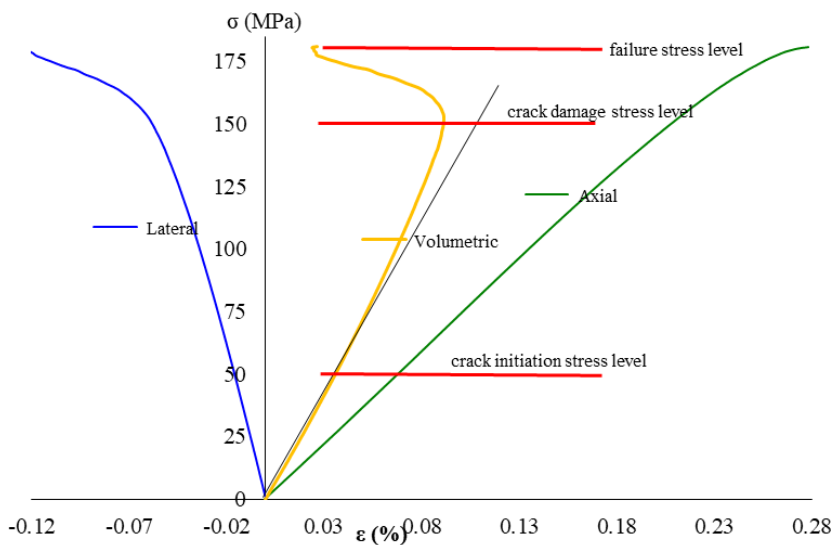


Figure 5: Axial stress–volumetric strain curve with the threshold of crack initiation and crack damage and failure stress for Hungarian granitic sample (uniaxial compression case).

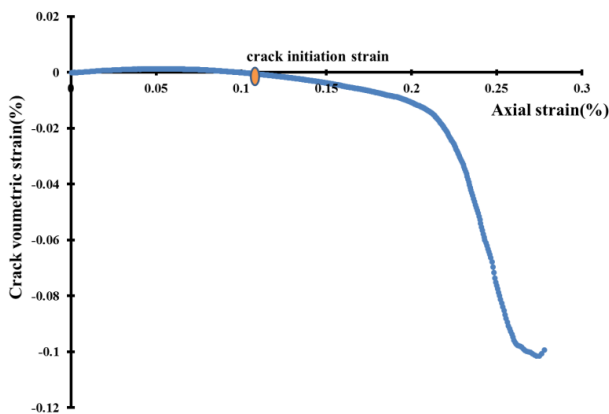


Figure 6: Crack volumetric strain method for crack initiation threshold determination for Hungarian granitic rock sample (uniaxial compression case).

Crack volumetric strain is calculated on the basis of these two elastic constants and is strongly sensitive to its value. This is probably why this method does not give objective values.

2.3 Change of Poisson’s ratio method

Diederichs [13] proposed a method of crack initiation threshold identification based on the change of Poisson’s ratio. The onset of crack initiation can be identified by the analysis of the relationship of Poisson’s ratio, evaluated locally, to the log of the axial stress (Fig. 7).

However, in this paper, the results obtained from the first method were used for further analysis. The reason is

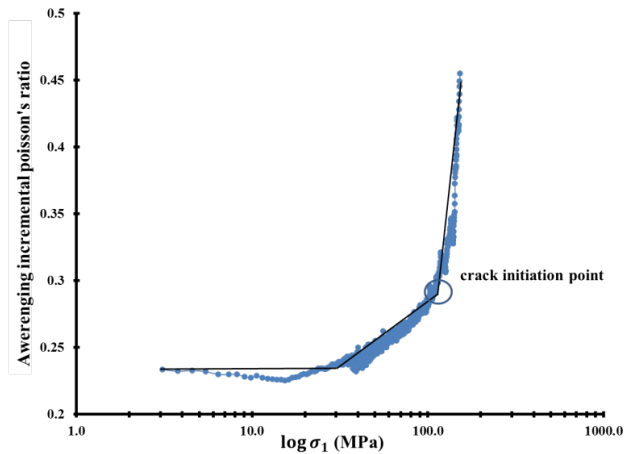


Figure 7: Poisson's ratio method for crack initiation threshold determination for Hungarian granitic rock sample (uniaxial compression case).

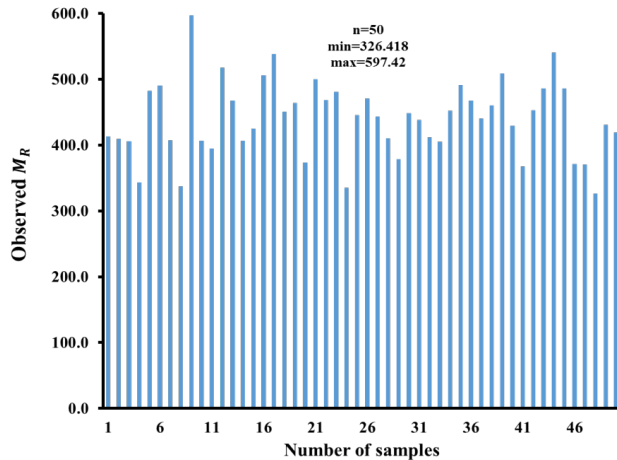


Figure 8: Observed values of modulus ratio (M_R) in each of 50 examined rock samples.

that, based on the findings by Cieslik [14], this method gives more precise results for granitic rock samples.

Table 1 also summarizes that the value of M_R in each of 50 studied granitic rock samples is between 326.4 and 597.4 with the mean of 439.4. The range of M_R obtained by Deere [15] is between 250 and 700 with the mean of 420 for limestone and dolomites. The range of M_R obtained by Palchik [7] is between 60.9 and 1011.4 with the mean value of 380.5 for carbonated rock samples. The mean value of M_R in this study is similar to the mean value of M_R obtained by Deere [15] and Palchik [7]. Fig. 8 shows the value of M_R for all studied samples in this study. As shown in Fig. 5, the range of $M_R=326.4-597.4$, observed in this study, is less than the range of M_R obtained by Deere [15] and Palchik [7].

The ranges of the elastic modulus (E), Poisson's ratio (ν), crack damage stress (σ_{cd}) and uniaxial compressive strength (σ_c), axial failure strain ($\varepsilon_{a, \max}$) and maximum volumetric strain (ε_{cd}), crack initiation stress (σ_{ci}) and crack initiation strain (ε_{ci}) for the studied 50 samples are presented as follows:

$$\begin{aligned} 57.425 \text{ GPa} < E < 88.937 \text{ GPa} \\ 0.18 < \nu < 0.32 \\ 30 \text{ MPa} < \sigma_{ci} < 90 \text{ MPa} \\ 77 \text{ MPa} < \sigma_{cd} < 182 \text{ MPa} \\ 133.34 \text{ MPa} < \sigma_c < 213.04 \text{ MPa} \\ 0.02 < \varepsilon_{ci} < 0.06 \\ 0.18 < \varepsilon_{a, \max} < 0.19 \\ 0.04 < \varepsilon_{cd} < 0.14 \end{aligned}$$

The ranges of $\frac{\varepsilon_{a, \max}}{\varepsilon_{cd}}$ and $\frac{\sigma_{cd}}{\sigma_c}$ and $\frac{\sigma_{ci}}{\sigma_c}$ ratios are 1.49–5.28 and 0.5–0.9 and 0.2–0.5, respectively. These values are different from the values of $\frac{\sigma_{cd}}{\sigma_c} = 0.5-1.0$ and $\frac{\varepsilon_{a, \max}}{\varepsilon_{cd}} = 1.51-6.91$ obtained by Palchik [7]. They are also different from the values of $\frac{\sigma_{ci}}{\sigma_c} = 0.71-0.84$ obtained by Brace et al. [11], Bieniawski [16], Martin [17], Pettitt et al. [18], Eberhardt et al. [19], Heo et al. [20] and Katz and Reches [21] for granites, sandstones and quartzites. The range of $\frac{\sigma_{ci}}{\sigma_c}$ for most rocks falls in the range of 0.3–0.5.

3 Effect of mechanical properties on M_R value

3.1 Relationship between M_R , σ_c and E for all granitic rock samples

The relationship between uniaxial compressive strength (σ_c), M_R and E is shown in Fig. 9. It illustrates that how uniaxial compressive strength influences M_R and E for all studied rock samples.

As it is clear, the elastic modulus is related to σ_c , with $R^2 = 0.06$ very small. It also demonstrates that increase in the value of σ_c from 133 to 213 MPa does not influence E value. It can be seen from Fig. 9 that M_R is related to σ_c , with $R^2 = 0.61$. These values, however, are different from the values found by Palchik [7] for carbonated rocks. In his studies, the elastic modulus is partly related to uniaxial compressive strength with $R^2 = 0.55$ and increase in the value of σ_c does not influence M_R value ($R^2 = 0.021$ is very small).

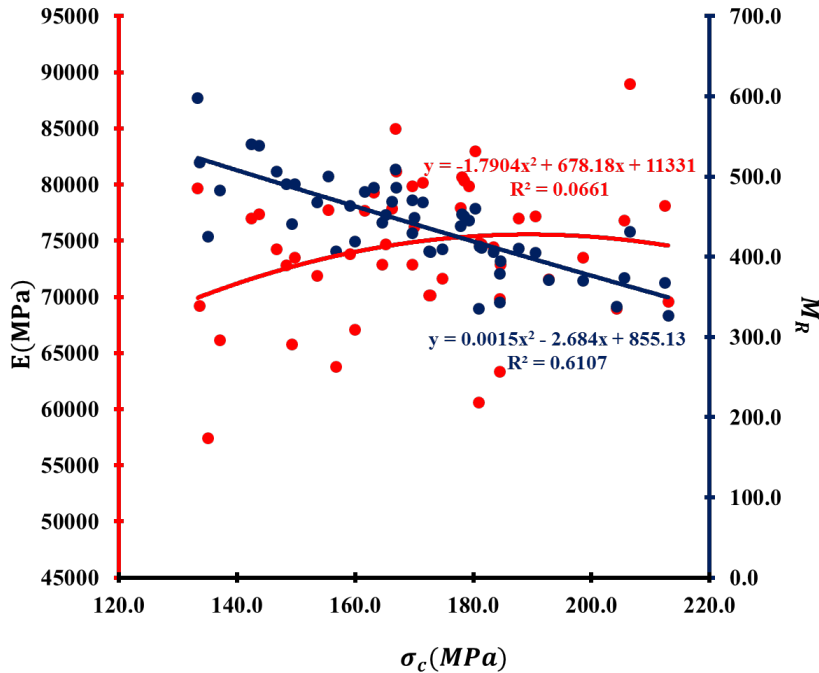


Figure 9: Influence of uniaxial compressive strength (σ_c) on elastic modulus (E) and the value of M_R for all studied samples.

3.2 Relationship between M_R value and different strain and stress of the rock

The calculated values are compared with the international published relationships.

$$\zeta_{(m)} = \frac{2 \left| \prod_{\text{obs}(j)} - \prod_{\text{cal}(j)} \right|}{\prod_{\text{obs}(j)} + \prod_{\text{cal}(j)}} \times 100 \quad (6)$$

3.2.1 Relationship between M_R and maximum axial strain ($\epsilon_{a, \text{max}}$) for all studied samples

The observed and analytical (Eq. 1) relationships between $\epsilon_{a, \text{max}}$ and M_R for all rock samples exhibiting $\epsilon_{a, \text{max}} < 1\%$ are plotted in Fig. 10. It is clear that the calculated Diederichs Eq. (1) and observed values of M_R for studied rock samples are similar. Fig. 11 presents the relative and root-mean-square errors between the calculated Diederichs Eq. (1) and observed M_R at $\epsilon_{a, \text{max}} < 1\%$. As it is clear, the relative error (ζ , %) for studied samples is between 0.28% and 25% and root-mean-square error is ($\chi = 50$). Comparing the values with the results obtained by Palchik [7] for carbonated rock samples, the relative error is between 0.08% and 10.8% and the root-mean-square error is 43.6.

The relative (ζ , %) and root-mean-square (χ) errors between the observed and calculated parameter Π have been calculated as:

$$\chi_{(m)} = \sqrt{\frac{\sum_{j=1}^n [\prod_{\text{obs}(j)} - \prod_{\text{cal}(j)}]^2}{n - 1}} \quad (7)$$

where $\prod_{\text{obs}(j)}$ is the observed value of parameter in the j th sample, here is M_R , $\prod_{\text{cal}(j)}$ is the calculated value of parameter in the j th sample, $j = 1, 2, \dots, n$, is the number of tested samples, here is 50.

3.2.2 Relationship between M_R and maximum volumetric strain ϵ_{cd} for all studied samples

The observed values between M_R and ϵ_{cd} are plotted in Fig. 12. As it is clear, these parameters are partially related ($R^2 = 0.2$) for studied rock samples. Palchik [7] however, found a good relationship ($R^2 = 0.85$) between these two parameters for carbonated rock samples.

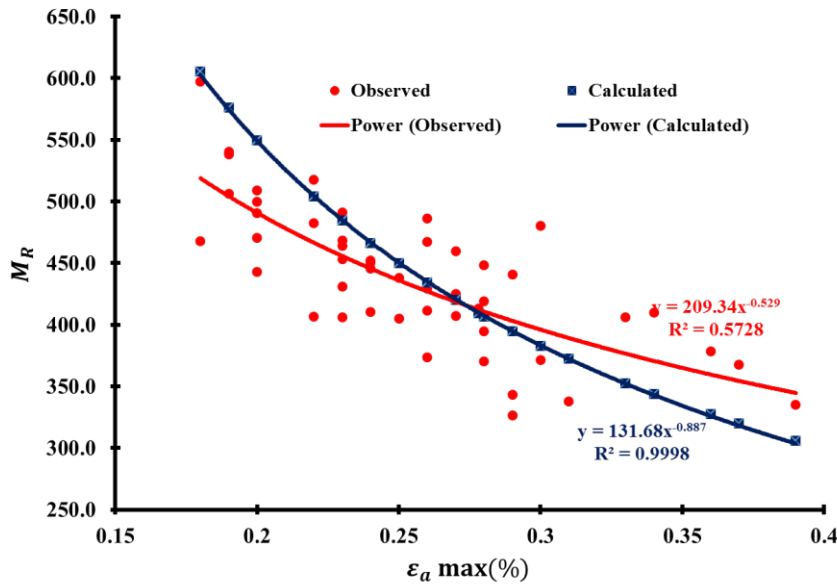


Figure 10: Observed and analytical (Eq. 1) relationship between $\varepsilon_{a, \max}$ and M_R .

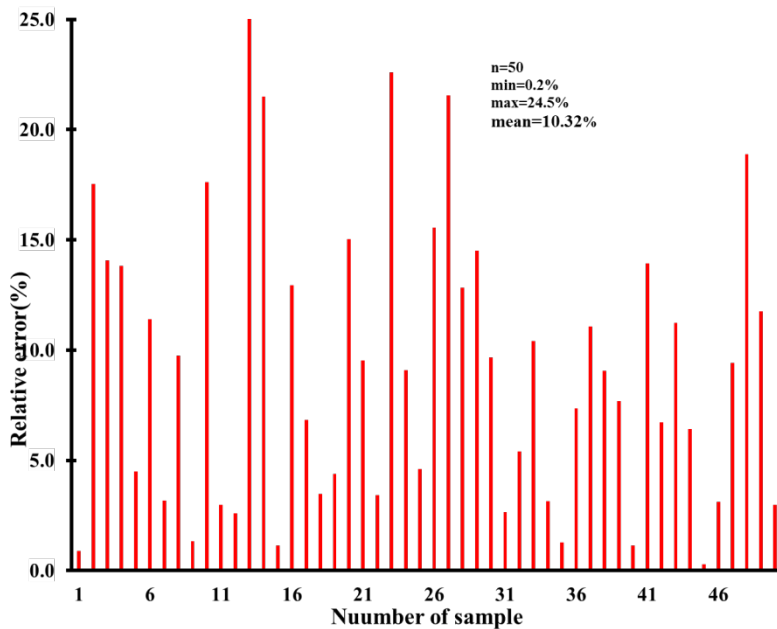


Figure 11: Relative (ε , %) and root-mean-square (χ) errors between calculated (Eq. 1) and observed M_R .

3.2.3 Relationship between M_R and crack damage stress s_{cd} for all studied samples

Fig. 13 shows the relationship between M_R and crack damage stress (σ_{cd}) for all studied rock samples. As it can be seen, there is a relationship ($R^2 = 0.41$) between these two parameters.

3.2.4 Relationship between M_R and $\frac{\sigma_{cd}}{\sigma_c}$ for all studied samples

The relationship between M_R and $\frac{\sigma_{cd}}{\sigma_c}$ is presented in Fig. 14. As it can be seen, there is practically no relationship ($R^2 = 0.0009$) between them.

3.2.5 Relationship between M_R and $\frac{\varepsilon_{a,max}}{\varepsilon_{cd}}$ for all studied samples

As shown in Fig. 15, there is practically no correlation between these two values.

3.2.6 Relationship between $\frac{\sigma_{cd}}{\sigma_c}$ and $\frac{\varepsilon_{a,max}}{\varepsilon_{cd}}$ for all studied samples

The relationship between $\frac{\sigma_{cd}}{\sigma_c}$ and $\frac{\varepsilon_{a,max}}{\varepsilon_{cd}}$ is presented in Fig. 16. As it can be seen, there is a relationship ($R^2 = 0.4$). Palchik [22], however, found the relationship ($R^2 = 0.7$) for carbonated rock samples.

3.2.7 Relationship between M_R and crack initiation stress (σ_{ci})

The relationship between M_R and crack initiation stress (σ_{ci}) is presented in Fig. 17. As it can be seen, there is practically no relationship between them ($R^2 = 0.08$).

3.2.8 Relationship between M_R and crack initiation strain (ε_{ci})

Fig. 18 shows the relationship between M_R and crack initiation strain (ε_{ci}). As it is shown, there is a relationship ($R^2 = 0.13$).

3.2.9 Relationship between M_R and $\frac{\sigma_{ci}}{\sigma_{cd}}$

Fig. 19 presents the relationship between M_R and $\frac{\sigma_{ci}}{\sigma_{cd}}$. As it is clear, there is practically no relationship ($R^2 = 0.03$).

3.2.10 Relationship between M_R and $\frac{\varepsilon_{ci}}{\varepsilon_{cd}}$

Fig. 20 shows the relationship between M_R and $\frac{\varepsilon_{ci}}{\varepsilon_{cd}}$. As it can be seen, there is practically no relationship ($R^2 = 0.06$).

3.2.11 Relationship between $\frac{\sigma_{ci}}{\sigma_{cd}}$ and $\frac{\varepsilon_{cd}}{\varepsilon_{ci}}$

Fig. 21 shows the relationship between $\frac{\sigma_{ci}}{\sigma_{cd}}$ and $\frac{\varepsilon_{cd}}{\varepsilon_{ci}}$. As it can be seen, there is a relationship ($R^2 = 0.54$).

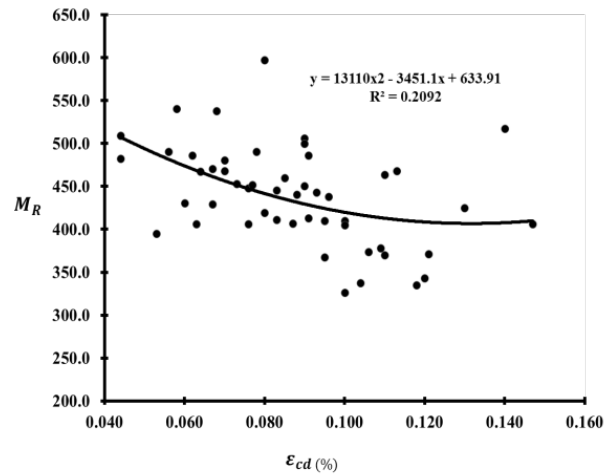


Figure 12: Relationship between M_R and ε_{cd} (%).

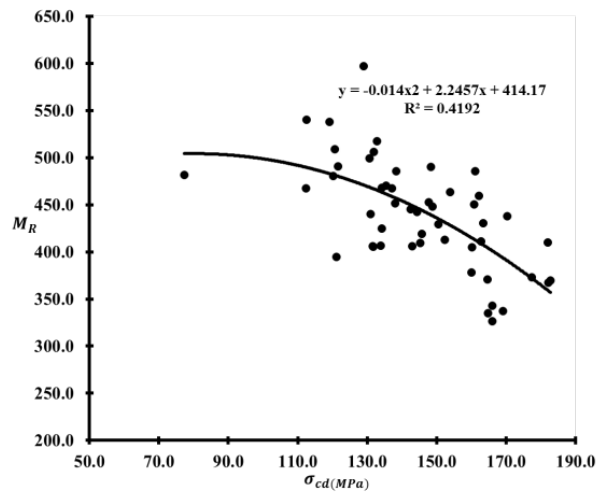


Figure 13: Relationship between M_R and σ_{cd} .

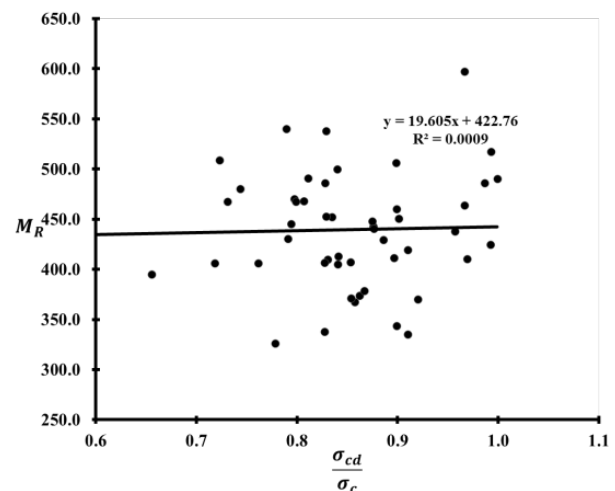


Figure 14: Relationship between M_R and $\frac{\sigma_{cd}}{\sigma_c}$.

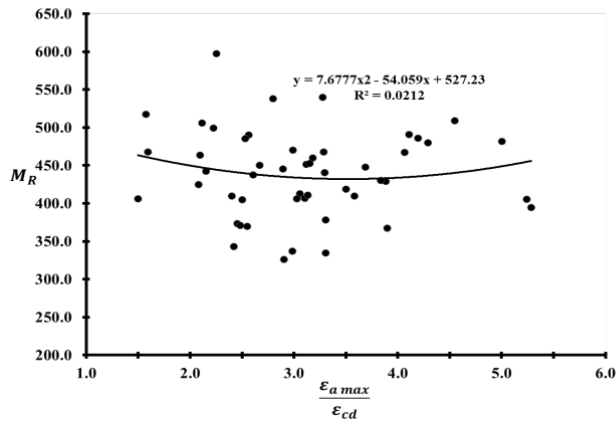


Figure 15: Relationship between M_R and $\frac{\varepsilon_{a,max}}{\varepsilon_{cd}}$.

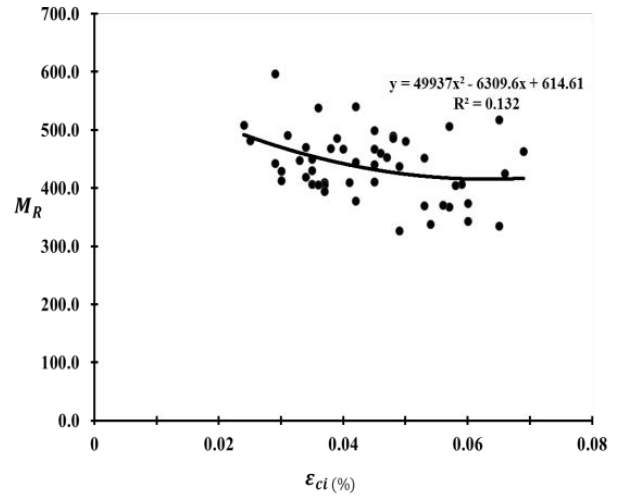


Figure 18: Relationship between M_R and crack initiation strain (ε_{ci}).

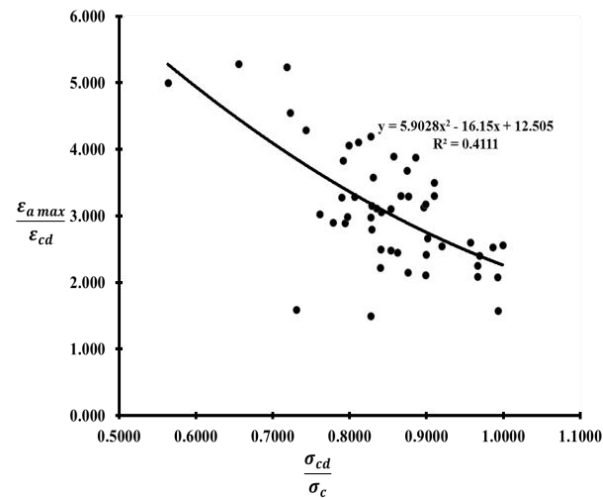


Figure 16: Relationship between $\frac{\sigma_{cd}}{\sigma_c}$ and $\frac{\varepsilon_{a,max}}{\varepsilon_{cd}}$.

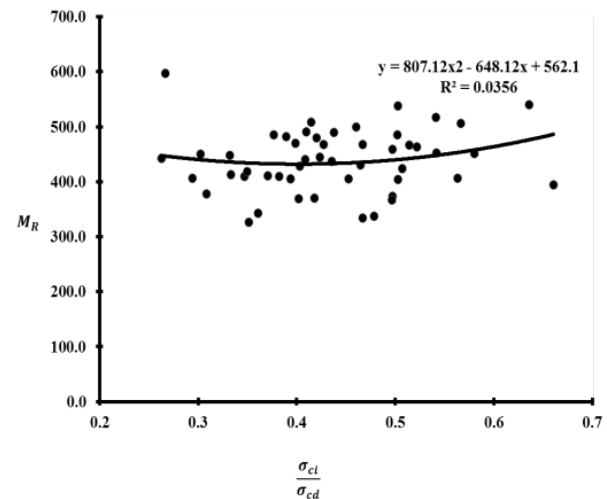


Figure 19: Relationship between M_R and $\frac{\sigma_{ci}}{\sigma_{cd}}$.

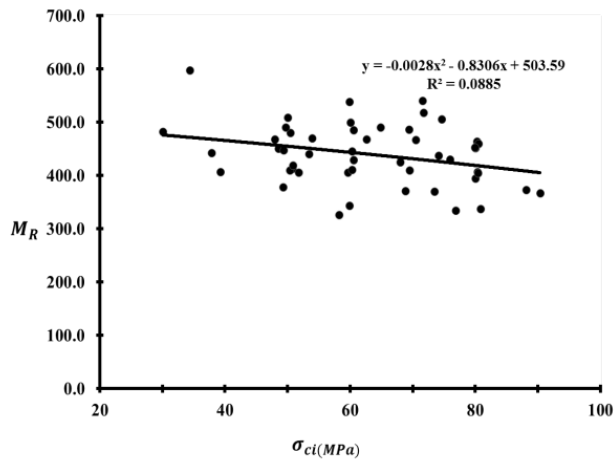


Figure 17: Relationship between M_R and crack initiation stress (σ_{ci}).

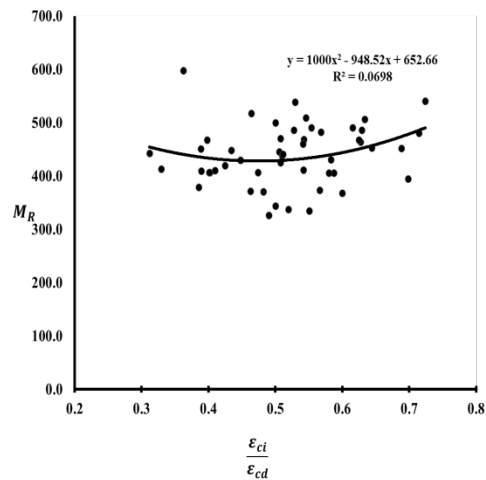


Figure 20: Relationship between M_R and $\frac{\varepsilon_{ci}}{\varepsilon_{cd}}$.

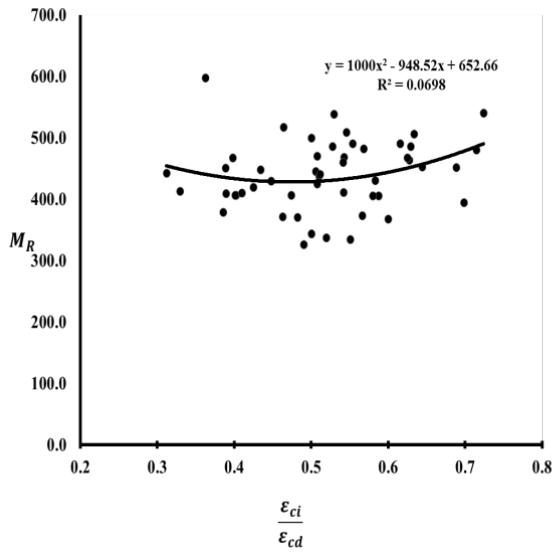


Figure 21: Relationship between $\frac{\sigma_{cd}}{\sigma_c}$ and $\frac{\epsilon_{ci}}{\epsilon_{cd}}$.

4 Results and discussions

The laboratory compressive tests, statistical analysis and empirical and analytical relationships have been used to estimate the values of $M_R = E/\sigma_c$ and its relationship with other mechanical parameters for granitic rocks. Studied rock samples exhibited the wide range of mechanical properties ($57.425 \text{ GPa} < E < 88.937 \text{ GPa}$, $0.18 < \nu < 0.32$, $77.3 \text{ MPa} < \sigma_{cd} < 212.42 \text{ MPa}$, $133.34 \text{ MPa} < \sigma_c < 213.04 \text{ MPa}$, $0.18 < \epsilon_{a\max} < 0.19$, $0.04 < \epsilon_{cd} < 0.14$). From the results of this study, the following main conclusions are made:

- The mean value of $M_{R\text{ mean}} = 439$ for all granitic rock samples observed in this study and the mean value of $M_{R\text{ mean}} = 420$ obtained by Deere [15] for limestone and dolomite and the mean value of $M_{R\text{ mean}} = 380.5$ obtained by Palchik [7] for carbonated rock samples are similar. However, the range of $M_R = 326.42\text{--}597.42$ obtained in this study is narrower than the range of $M_R = 250\text{--}700$ obtained by Deere [15] and the range of $M_R = 60\text{--}1,600$ obtained by Palchik [7].
- The observation confirms that there is no general empirical correlation (with reliable R^2) between elastic modulus (E) and uniaxial compressive strength (σ_c), M_R and maximum volumetric strain (ϵ_{cd}), M_R and crack damage stress σ_{cd} .
- The analytical relationship (Eq. 1) between $\epsilon_{a\max}$ and M_R offered by Palchik [7] or carbonated rock samples was investigated for granitic rock samples in this study. It is observed that this relationship can also be used for granitic rocks. The relative error (ζ , %) for studied samples is between 0.2% and 24.5% and root-

mean-square error is ($\zeta = 50$). Comparing the values with the result obtained by Palchik [7] for carbonated rock samples, the relative error is between 0.08% and 10.8% and the root-mean-square error is 43.6.

- The observed correlation between M_R and ϵ_{cd} for studied granitic rock sample is $R^2 = 0.2$. Palchik [7], however, found a good relationship ($R^2 = 0.85$) between these two parameters for carbonated rock samples.
- It is established that there is a correlation between $\frac{\sigma_{ci}}{\sigma_{cd}}$ and $\frac{\epsilon_{cd}}{\epsilon_{ci}}$ with $R^2 = 0.54$.
 - Based on the obtained results, there is practically no relationship between M_R and $\left(\frac{\epsilon_{a\max}}{\epsilon_{cd}}\right)$, $\left(\frac{\sigma_{cd}}{\sigma_c}\right)$, (σ_{ci}) , $\left(\frac{\sigma_{ci}}{\sigma_{cd}}\right)$, $\frac{\epsilon_{cd}}{\epsilon_{ci}}$; however, there is a relationship between M_R and (ϵ_{cd}) , (σ_{cd}) and (ϵ_{ci}) .

Notably, for a more precise and fundamental description of the mechanical behaviour of rock, one should apply non-equilibrium continuum thermodynamics along the lines of Asszonyi et al. [23, 25] and beyond. These relationships can be used for determining the mechanical parameters of the rock mass, as well [24, 26].

Acknowledgements: This paper has been published with the permission of Public Limited Company for Radioactive Waste Management (PURAM). The project presented in this article is supported by National Research, Development and Innovation Office – NKFIH 124366 and NKFIH 124508 and the Hungarian-French Scientific Research Grant (No. 2018-2.1.13-TÉT-FR-2018-00012).

References

- [1] Vászárhelyi, B. (2005). Statistical analysis of the influence of water content on the strength of the Miocene limestone. *Rock Mechanics and Rock Engineering*, 38, 69-76.
- [2] Palchik, V., (2007). Use of stress-strain model based on Haldane's distribution function for prediction of elastic modulus. *International Journal of Rock Mechanics and Mining Sciences*, 44(4), 514-524.
- [3] Ocak, I. (2008). Estimating the modulus of elasticity of the rock material from compressive strength and unit weight. *Journal of the Southern African Institute of Mining and Metallurgy*, 108(10), 621-629.
- [4] Ramamurthy, T., Madhavi Latha, G., Sitharam, T.G. (2017). Modulus ratio and joint factor concepts to predict rock mass response. *Rock Mechanics and Rock Engineering*, 50, 535-366.
- [5] Deere, D., Miller, R. (1966). Engineering classification and index properties for intact rock. Techn. Report. No. AFWL-TR-65-116, Air Force
- [6] Palmström, A., Singh, R. (2001). The deformation modulus of rock masses - comparisons between in situ tests and indirect

- estimates. *Tunnelling and Underground Space Technology*, 16, 115-131.
- [7] Palchik, V. (2011). On the ratios between elastic modulus and uniaxial compressive strength of heterogeneous carbonate rocks. *Rock Mechanics and Rock Engineering*, 44, 121-128.
- [8] Vászárhelyi, B., Kovács, L., Kovács, B. (2013). Determining the failure envelope of intact granitic rocks from Bábaapáti. *GeoScience Engineering*, 2(4), 93-101.
- [9] Buda, Gy. (1985). Formation of Variscan collisional granitoids. (in Hungarian) Candidate thesis, Eötvös University, Budapest, Hungary.
- [10] Király, E. Koroknai, B. (2004). The magmatic and metamorphic evolution of the north-eastern part of the Mórág Block. Annual Report of Geological Institute of Hungary from 2003, pp. 299-318.
- [11] Brace, W.F., Paulding, B.W., Scholz, C. (1966). Dilatancy in the fracture of crystalline rocks. *Journal of Geophysical Research*, 71, 3939-3953.
- [12] Martin, C.D., Chandler, N.A. (1994). The progressive fracture of Lac du Bonnet granite. *International Journal of Rock Mechanics and Mining Sciences*, 31, 643-659.
- [13] Diederichs, M.S. (2007). The 2003 Canadian Geotechnical Colloquium: mechanistic interpretation and practical application of damage and spalling prediction criteria for deep tunnelling. *Canadian Geotechnical Journal*, 44, 1082-1116.
- [14] Cieslik, J. (2014). Onset of crack initiation in uniaxial and triaxial compression tests of dolomite samples. *Studia Geotechnica et Mechanica*, 1, 23-27.
- [15] Deere, D.U. (1968). Geological considerations. In: *Rock mechanics in engineering practice*. Edited by K.G. Stagg, O.C. Zienkiewicz., pp. 1-20.
- [16] Bieniawski, Z.T. (1967). Mechanism of brittle fracture of rock. *International Journal of Rock Mechanics and Mining Sciences*, 4, 395-430.
- [17] Martin, C.D. (1993). *Strength of massive Lac du Bonnet granite around underground openings*. PhD thesis, Department of Civil and Geological Engineering, University of Manitoba, Winnipeg.
- [18] Pettitt, W.S., Young, R.P., Marsden, J.R. (1998). Investigating the mechanics of microcrack damage induced under true-triaxial unloading. In: *Eurock 98, Society of Petroleum Engineering*, pp. SPE 47319.
- [19] Eberhardt, E., Stead, D., Stimpson, B. (1999). Quantifying progressive pre-peak brittle fracture damage in rock during uniaxial compression. *International Journal of Rock Mechanics and Mining Sciences*, 36, 361-380.
- [20] Heo, J.S., Cho, H.K., Lee, C.I. (2001). Measurement of acoustic emission and source location considering anisotropy of rock under triaxial compression. In: *Rock mechanics a challenge for society*. Edited by P. Sarkka, P. Eloranta . Swets and Zeitlinger Lisse, Espoo, pp. 91-96.
- [21] Katz, O., Reches, Z., (2004). Microfracturing, damage and failure of brittle granites. *The Journal of Geophysical Research*, 109(B1).
- [22] Palchik, V., (2013). Is there link between the type of the volumetric strain curve and elastic constants, porosity, stress and strain characteristics? *Rock Mechanics and Rock Engineering*, 46 , 315-326.
- [23] Asszonyi, Cs., Fülöp, T., Ván, P. (2015). Distinguished rheological models for solids in the framework of a thermodynamical internal variable theory. *Continuum Mechanics and Thermodynamics*, 27(6), 971-986. doi: 10.1007/s00161-014-0392-3.
- [24] Vászárhelyi, B., Kovács, D. (2017). Empirical methods of calculating the mechanical parameters of the rock mass. *Periodica Polytechnica Civil Engineering*, 61(1), 39-50.
- [25] Asszonyi, Cs., Csátár, A., Fülöp, T. (2016). Elastic, thermal expansion, plastic and rheological processes – theory and experiment. *Periodica Polytechnica Civil Engineering*, 60(4), 591-601.
- [26] Vászárhelyi, B., Davarpanah, M. (2018). Influence of water content on the mechanical parameters of the intact rock and rock mass. *Periodica Polytechnica Civil Engineering*, 62(4), 1060-1066.